INTERNATIONAL JOURNAL OF CONSERVATION SCIENCE

ISSN: 2067-533X Volume 15, Issue 2, 2024: 815-828 www. ijcs. ro

DOI: 10. 36868/IJCS.2024.02.05

EFFECT OF ACOUSTIC WAVES CAUSED BY BELLS ON A STAINED-GLASS WINDOW

Dawid CEKUS[1*], Sebastian GARUS[1], Marcin NABIAŁEK[2], Maciej NADOLSKI[2], Piotr PASZTA[1]

[1] Faculty of Mechanical Engineering and Computer Science, Czestochowa University of Technology, Armii Krajowej 21 Av., 42-200 Częstochowa, Poland

[2] Faculty of Production Engineering and Materials Technology, Czestochowa University of Technology, Armii Krajowej 19 Av., 42-200 Częstochowa, Poland

Abstract

The paper presents the influence of acoustic waves caused by bells on a stained-glass window and its components. The issue is particularly important in the context of church towers with bells and stained-glass windows. The free vibrations of a sample stained-glass window were analyzed numerically, with changes related to the thickness of the glass used and the parameters of the lead cames that form the internal metallic structure of a window panel. The obtained results can be generalized to any other sources of acoustic waves and they can constitute the basis for determining the properties of the designer of stained-glass window or introducing additional barriers to avoid the phenomenon of resonance.

***Keywords**: Acoustic waves; Bells; Stained-glass window; Natural frequency; FEM*

Introduction

Stained-glass is a type of decorative window filling, made of fragments of colored glass connected together using a copper foil covered with tin (Tiffany technique) or C- or H-shaped lead came (traditional technique), the contacts of which are soldered and the whole is mounted between metal bars. The origins of stained-glass date back to ancient times, but their heyday and beginning in Europe fell on the Middle Ages (10th century). The renaissance of stained-glass took place at the turn of the 19th and 20th centuries.

Originally, stained-glass windows were placed in religious buildings and often depicted biblical scenes and characters. Currently, they are still used as decorations in temples, but they can also be utilized as decorations in any public building or in any home.

The size of a stained-glass window can be any, but the mechanical properties make it necessary to divide the window surface into sections that can be given appropriate stiffness and can be manipulated during installation. The size of individual stained-glass window should not exceed 600 x 800 mm, otherwise it must be additionally reinforced, as over time it may deform under their own weight.

Stained-glass windows are exposed to various factors that have a destructive effect on both glass elements and lead cames [1, 2]. Factors that have a harmful effect on stained glass include: moisture condensation (increases corrosion), air pollution (mainly sulphur dioxide), microbiological factors (microorganisms, algae and fungi) and mechanical factors (wind

* Corresponding author: dawid.cekus@pcz.pl

pressure, vibrations caused by street and air traffic [3] or construction works [4], noise generated by mass events [5]). Atmospheric factors act particularly strongly on the outside of stained-glass, but inside objects the delicate structures of stained glass are also exposed to impacts that have not been widely considered in the literature so far. Namely, these are vibrations caused by acoustic waves that arise from the ringing of bells. Of course, the stained-glass windows are not placed in the immediate nearness of the bells, which need an open space for the sound to spread, but in extreme cases such proximity is likely. While at first glance it may seem that stained glass-windows are immune to this type of acoustic pollution, in fact even moderate noise levels can have a negative impact on their condition and integrity. Therefore, in this paper, an attempt was made to verify this thesis and check the impact of acoustic waves caused by bells on physical objects located near them. For this purpose, a rib (transverse profile of the bell) was used, which was obtained during 3D scanning of an object (Fig. 1) located in one of the churches in Kudirkos Naumiestis (Lithuania). On this basis, a scaled geometric model was prepared and a reduced copy of the original weighing approximately 25 kg was casted (according to the numerical model).

Fig. 1. Bells on the tower in one of the churches in Kudirkos Naumiestis (Lithuania) (on the left) and the process of scanning one of them (on the right)

Numerical studies

The numerical tests used the ANSYS software [6, 7, 8, 9], in which the vibrations of the bell and the impact of the acoustic wave on the glass (simplification of the stained glass-window) were analyzed, as well as the SolidWorks program [10, 11], in which obtained the frequencies and modes of vibrations of the stained-glass window. This division of tasks allowed for the simplification of simulation models and acceleration of computations without affecting their quality. Table 1 compiles the basic material parameters that were used in both programs during all numerical calculations. In the case of glass, the default material parameters from both programs were adopted, therefore there are differences between their values in Table 1.

Table 1. Parameters of materials used in numerical analyses

Software	ANSYS		SolidWorks		
Material	**Bronze**	**Glass**	**Steel AISI 304**	**Lead**	**Glass**
Elastic Modulus [MPa]	110000	69930	190000	14000	68935
Poisson's Ratio	0.341	0.21	0.29	0.4	0.23
Mass Density [kg/m^3]	8802	2465	8000	11000	2457.6

Numerical analysis of the bell

The first stage of the work was to develop a solid geometrical model (on the basis of the rib from 3D scan) and a computational model of the bell (Fig. 2) and to determine its acoustic properties with the help of finite element method (FEM). The mesh density in the computational model was adopted using the automatic method with a maximum finite element size of 5 mm. It was assumed that the bell is made (like the casted bell) of C91300 bell bronze [12] (Table 1 - Bronze).

Fig. 2. Geometrical model (on the left) and its mesh (element size: 5mm, nodes: 388078, elements: 203650) (on the right)

The sound emitted by the bell consists of the sum of its individual partials and residual noise [13-15], therefore only the identified basic sound components are indicated in Table 2, and the corresponding vibration modes in Figure 3. The ideal relation between the five basic sound partials hum: fundamental: tierce: quint: nominal are defined by the following dependence: 1, 1:2, 1:2.4, 1:3, 1:4 [14]. In reality, it is not possible to achieve such relations and, for example, for tierce the multiplier changes with the mass of the bell and requires adjustment to the musical frequency of the sound. The difference between the theoretical and real sound of the bell is influenced by its ornamentation, which changes the local thickness of the cross-section, and the casting process with defects in the form of porosity inside the bell material (Table 2).

Table 2. Sound partials and vibration frequencies of the analyzed bell.

Partial	Numerical frequency [Hz]	Musical/theoretical frequency [Hz]	Sound
Hum	589.99	587,32	d^2
Fundamental	1185.8	1174,65	d^3
Tierce	1413.9	1396,91	f^3
Quint	1773.8	1760,00	a^3
Nominal	2376.5	2349,31	d^3

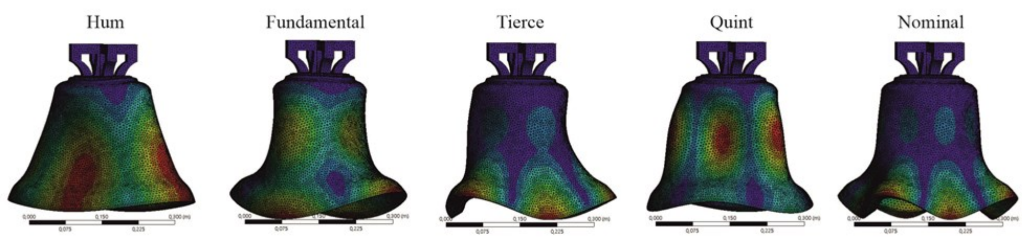

Fig. 3. Modal shapes for the musical partials of an analyzed bell predicted by FEM

Numerical analyses of acoustic wave in space

The second stage of the research was the analysis of the acoustic wave in space that affects the object, in the examined case a stained-glass window. In the numerical analysis, in order to shorten and simplify calculations, the stained-glass window was replaced with a homogeneous pane of soda-lime glass (Table 1 – ANSYS/Glass) with dimensions of 500 mm x 500 mm x 2 mm and the mass of 1.23 kg. The computational model is shown in Figure 4. It is assumed that the acoustic wave propagates in an elastic medium (air) with the following parameters: speed of sound 346.25 m/s, viscosity $1.7894 \cdot 10^{-5}$ Pa·s, density 1.225 kg/m^3. It should be mentioned that acoustic analysis is not a typical fluid analysis. Sound is created by moving pressure waves that carry energy through a medium, but not by a moving mass (in acoustic analysis, air does not flow).

Meshing is an extremely important factor in acoustics simulations since it strongly affects the accuracy of the obtained results. Suitable high quality meshing is required to get accurate and reliable answers. Therefore, the mesh element size for air was assumed to be 11 mm (the increasing the mesh density does not significantly improve the results of computation).

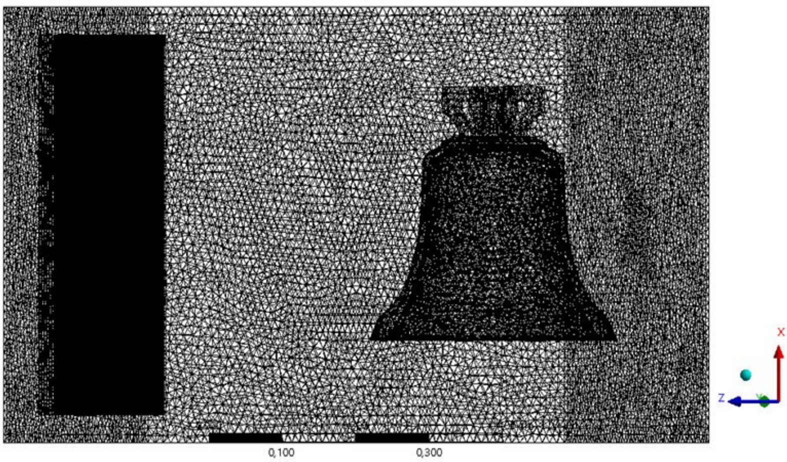

Fig. 4. Meshed fluid domain the near-field, air, nodes: 2489322, elements: 1783013

The tests carried out in the near-field mesh domain allowed to obtain the distribution of sound pressure level (SPL) in the fluid (air) (Fig. 5a) and acoustic pressure (Fig. 5b) for selected frequencies: 589.99 Hz, 1185.8 Hz, 1413.9 Hz, 1773.8 Hz, and 2376.5 Hz. At the same frequencies, a total deformation of the glass imitating stained-glass was also calculated (Fig. 6).

Additionally, a detailed analysis of the acoustic wave spectrum was performed in the full frequency range from 0 to 2500 Hz (including all previously determined basic partials of the bell sound) at three measurement points. The first measurement point (microphone) was placed right next to the bell (Fig. 7a), the second (Fig. 7b) and the third point (Fig. 7c) were located just in front of and behind the glass, respectively. Figure 8 shows the measured SPL values.

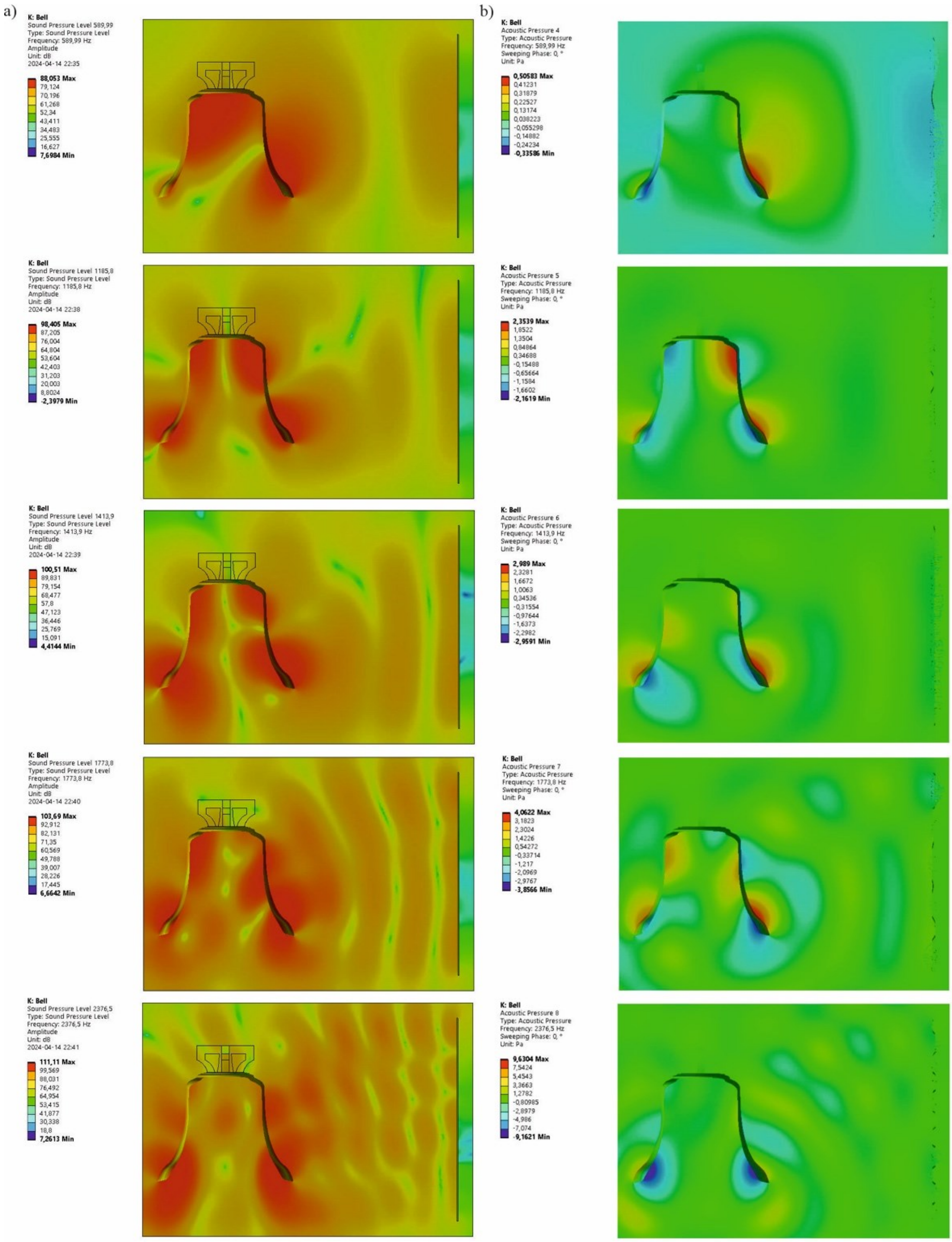

Fig. 5. Sound pressure level in dB (a) and acoustic pressure in Pa (b) at: 589.99 Hz, 1185.8 Hz, 1413.9 Hz, 1773.8 Hz, 2376.5 Hz

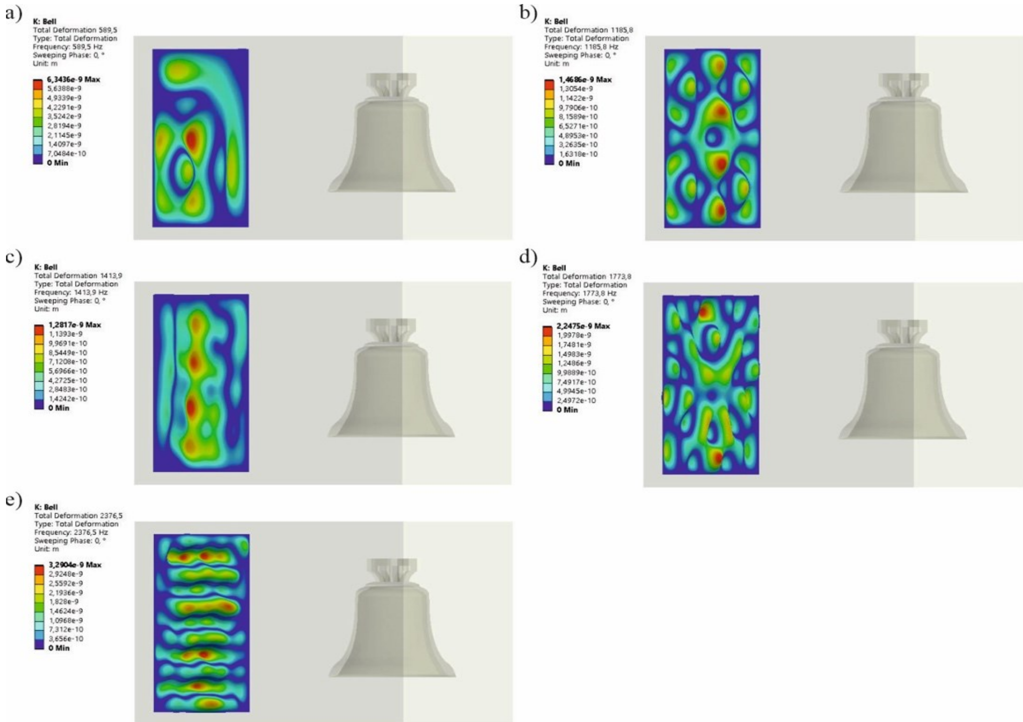

Fig. 6. Total deformation of the glass

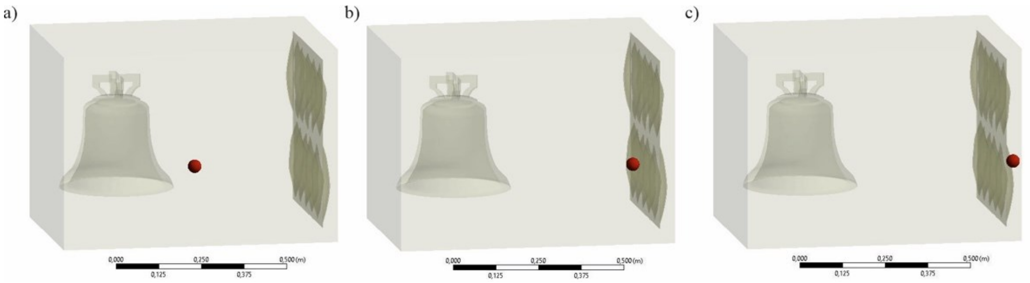

Fig. 7. Positions of microphone: a) Mic 1, b) Mic 2, c) Mic 3

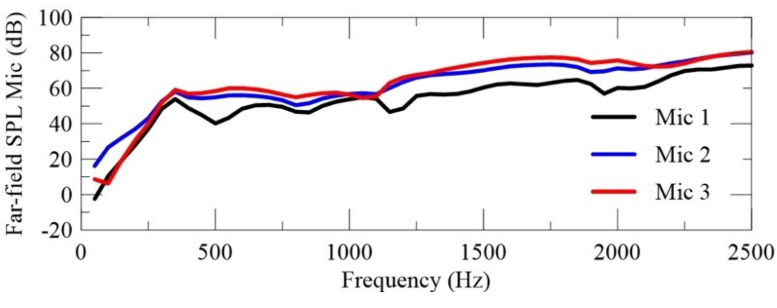

Fig. 8. SPL measured in the three points in the range from 0 to 2500 Hz

Numerical analyses of stained-glass

The next stage of the research was the analysis of the vibrations of the stained-glass window. Numerical tests were executed for three models. The first model was a uniform glass. The second model was a simplified stained glass-window (Fig. 9a), i.e. containing fewer detailed divisions of glass. The third model was a classic stained-glass window (Fig. 9b). This division of tasks was intended to show changes in the frequency and amplitude of vibrations of individual objects. The geometrical models were prepared in SolidWorks and parameterized in such a way as to enable a problem-free analysis of the influence of the glass thickness (parameter *a* in Fig. 10) on the searched values.

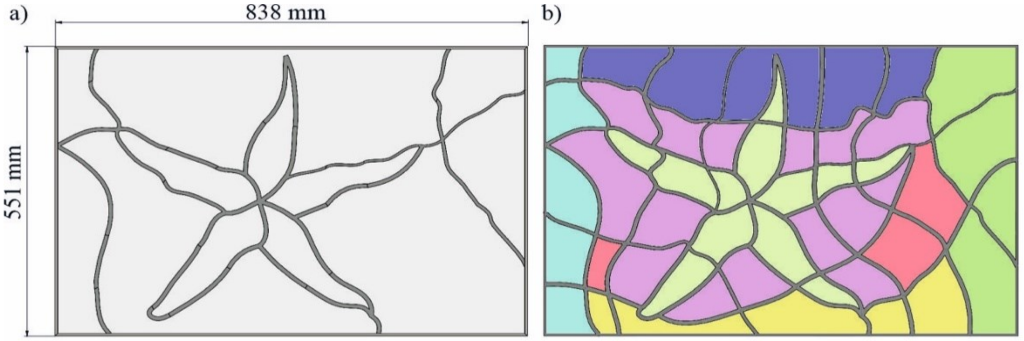

Fig. 9. Geometrical models: a) the simplified stained-glass, b) the full stained-glass

The considered size of the panel (in this case the examined stained-glass window) is 838 mm x 551 mm. It was assumed that the maximum width of the lead came is 8 mm. The glass is perfectly mounted (with no space for sealant, which is pressed into the gaps) and inserted into the frame by a maximum of 3 mm. In the FEM computational model, all degrees of freedom on the external surfaces of the steel frame were taken away, as if the stained-glass window was fixed in the wall opening.

Tables 3÷5 list the first six vibration frequencies of the glass (Table 3), simplified stained-glass (Table 4) and full stained-glass (Table 5), with different thicknesses of the used glass. Moreover, Figure 11 shows the modes corresponding to the vibration frequencies of a full stained-glass window with a glass thickness of 3 mm. Figure 11a illustrates additionally the finite element mesh accepted.

Table 3. The first six vibration frequencies of the glass at different thicknesses of glass used

Thickness of glass (a) [mm]	Frequency [Hz]					
	Mode 1	Mode 2	Mode 3	Mode 4	Mode 5	Mode 6
3	66.76	102.07	161.84	164.15	197.07	244.55
4	88.61	135.52	214.93	217.79	261.49	324.76
5	110.39	168.87	267.84	271.20	325.65	404.69
6	132.05	202.08	320.57	324.27	389.43	484.31

Table 4. The first six vibration frequencies of a simplified stained-glass window with different thicknesses of glass used.

Thickness of glass (a) [mm]	Frequency [Hz]					
	Mode 1	Mode 2	Mode 3	Mode 4	Mode 5	Mode 6
3	59.62	94.25	146.46	151.56	185.27	224.59
4	80.18	126.27	196.68	202.95	247.50	300.85
5	100.66	158.14	246.69	254.09	309.38	376.79
6	121.03	189.86	296.40	304.90	370.86	452.21

Table 5. The first six vibration frequencies of a full stained-glass window at different thicknesses of glass used.

Thickness of glass (a) [mm]	Frequency [Hz]					
	Mode 1	Mode 2	Mode 3	Mode 4	Mode 5	Mode 6
3	56.26	86.91	138.36	139.33	168.30	209.20
4	75.94	117.19	186.46	187.78	226.66	281.79
5	95.57	147.37	234.42	236.06	284.80	354.13
6	115.11	177.41	282.11	284.07	342.59	426.02

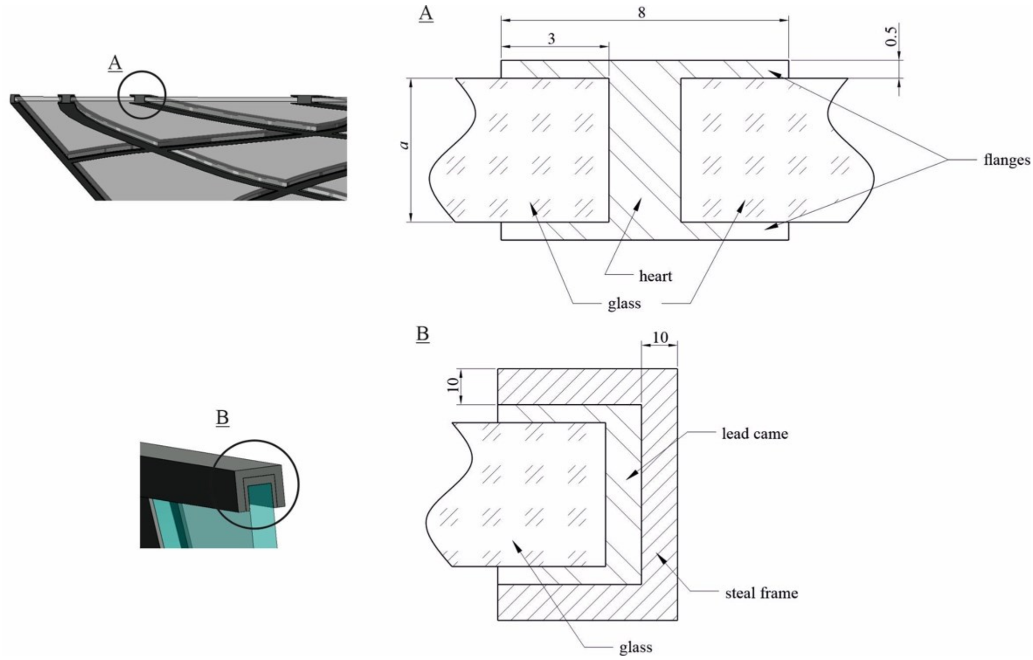

Fig. 10. Parameters of lead cames and steel frame

The paper did not include subsequent vibration modes for other glass thicknesses and other models, because their shape was practically identical, with the difference that the resultant amplitude decreases with increasing glass thickness. Similarly, the vibration amplitude decreases with an increased number of lead cames in the stained-glass window, as shown in Table 6.

Table 6. Resultant amplitudes for the analyzed models, with a glass thickness of 3 mm.

Type of model	**AMPRES: Resultant amplitude**					
	Mode 1	**Mode 2**	**Mode 3**	**Mode 4**	**Mode 5**	**Mode 6**
Panel of glass	1.330	1.270	1.252	1.233	1.211	1.242
Simplified stained-glass	1.204	1.226	1.211	1.422	1.254	1.167
Full stained-glass	1.124	1.089	1.088	1.152	1.078	1.088

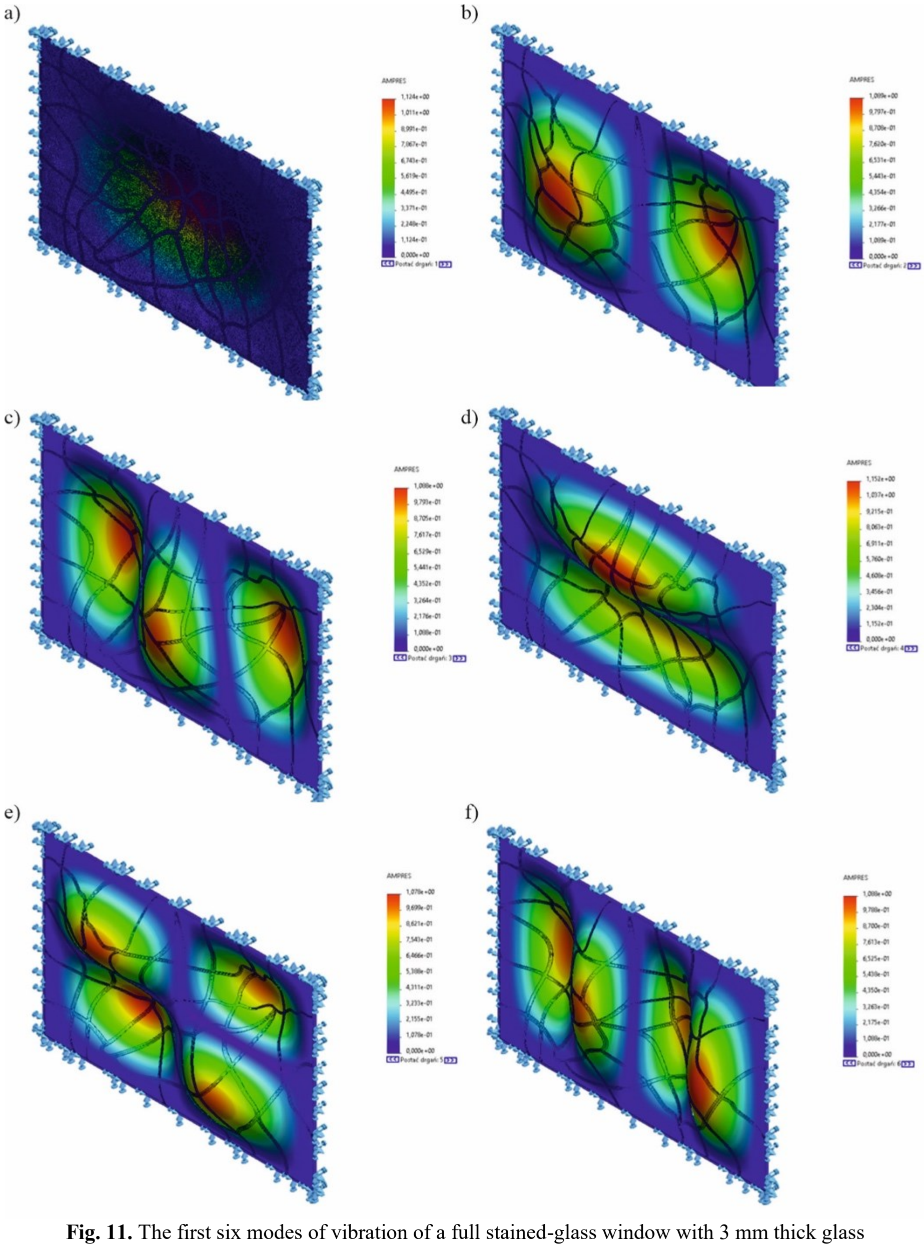

Fig. 11. The first six modes of vibration of a full stained-glass window with 3 mm thick glass

Experiment

Since numerical models are often unable to fully reflect real objects and conditions, experimental research are conducted. As part of this work, acoustic tests were performed on the bell (Fig. 12e), which was casted (Fig. 12d) in mold (Fig. 12c) printed from sand and resin. Although 3D printing is now generally available and is becoming popular for unit castings, it is still new in bell founding. Mold models (Fig. 12b) were prepared on the basis of the analyzed geometrical model, taking into account the technological properties of bell bronze (shrinkage), which occurs during the solidification process of the casting in the mold.

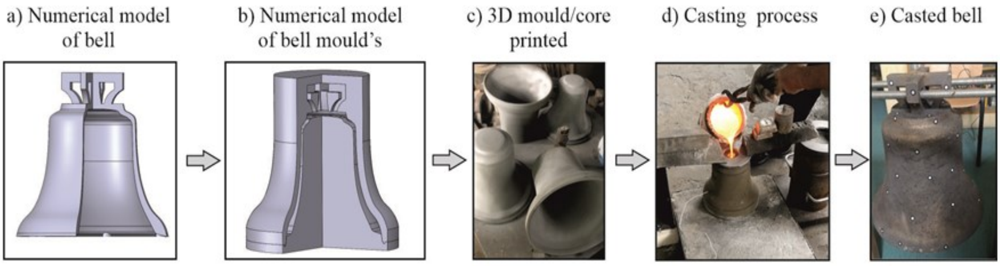

Fig. 12. The process of preparing a bell for experimental tests

Methods

The frequency spectrum was determined using an electret, omni-directional UMIK-1 measurement microphone. The frequency range from 20 Hz to 20 kHz was analyzed with an accuracy of +/- 1 dB, with a sampling rate of 48 kHz and a resolution of 24 bits. Figure 13 shows the maximum sound pressure level values for the bell in the spectrum range up to 4 kHz. The first natural frequency f_1 was 570.92 Hz and was marked in the figure with the first vertical line on the left. Subsequent vertical lines are marked for subsequent harmonics $f_n = n{\cdot}f_1$.

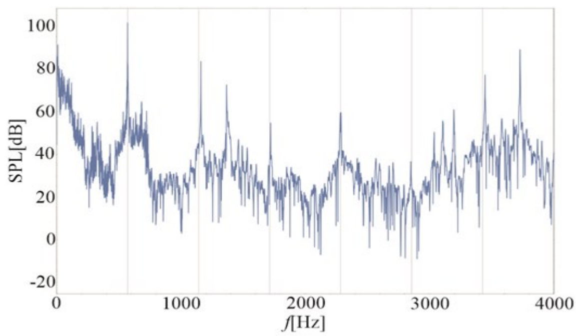

Fig. 13. Spectrum of maximum sound pressure level (SPL) values for the bell

Table 7 presents the frequency values and the corresponding sound pressure level values of peaks occurring in the spectrum range up to 4 kHz.

Table 7. Frequencies and corresponding values of the sound pressure level that make up the sound timbre of the analyzed bell.

	f [Hz]	SPL [dB]
f_1	570.9	101.8
f_2	1161.9	83.9
	1360.0	72.7
f_3	1721.9	54.4
f_4	2285.7	59.6
f_5	2845.7	36.7
	3036.2	50.5
	3108.6	55.6
	3196.2	61.2
f_6	3447.6	77.1
	3729.5	88.8

Figure 14 shows changes in the bell sound spectrum over time. In the analyzed time period of 15 seconds, the first natural frequency did not have time to extinguish. The second natural frequency sounded for 8 seconds, and the subsequent timbre components finished their vibrations in less than 4 seconds.

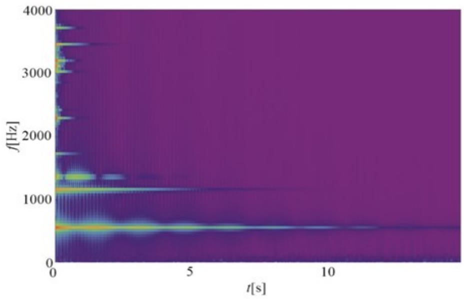

Fig. 14. Spectrum of maximum sound pressure level (SPL) values for the bell

Discussion

When comparing the acoustic properties of the bell obtained from simulation and experimental tests, some differences are noted. Firstly, the values of the vibration frequencies of the sound components differ from each other, which is a consequence of the idealized numerical model. The assumed boundary conditions and material distribution in the computational model can never be reproduced in real conditions [16, 17]. However, the relative error between the numerical and experimental frequencies does not exceed 4%, which is within the norms. Moreover, in experimental studies the vibration frequency of 1360.0 Hz was not identified as a sound partial (harmonic), which in the numerical model is a Tierce (1413.9 Hz).

The SPL obtained numerically and experimentally is difficult to compare. First of all, the place of measurement was different. In the case of simulation tests in the ANSYS program, it was assumed that the bell was excited by a force of 50N, while during tests on a real object, the bell was hit with a metal ball from the outside and the excitation force was not measured. Additionally, the excitation point in both cases was not identical, although attempts were made to make it as close as possible. In spite of this, it can be presumed from both studies that the maximum SPL does not exceed 112 dB numerically and 102 dB experimentally. This gives the maximum acoustic pressure of approximately 10 Pa (Fig. 5) with which the bell can affect objects in the immediate vicinity. The further the object is from the sound source, the lower this value is. Nevertheless, a static analysis was performed in the SolidWorks program of a full stained-glass window loaded with a pressure of 10 Pa on its entire surface. The get results illustrated in Figure 15 indicate that under such boundary conditions, the stained-glass elements displacement by a maximum of 0.003 mm and are not exposed to excessive stresses and strains. All this means that the acoustic force does not have a significant impact on the possibility of damaging the stained glass window.

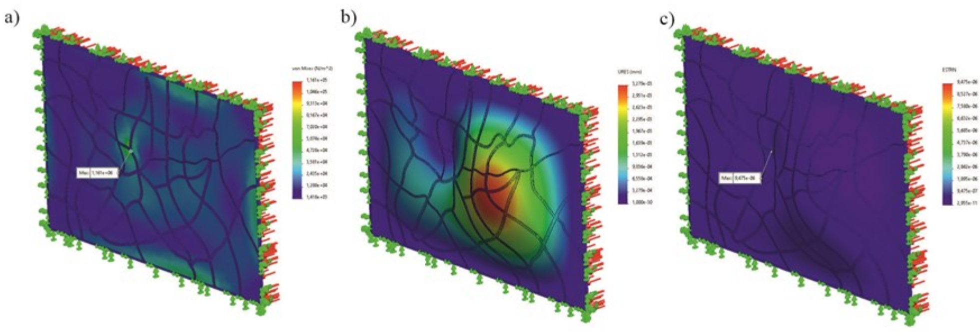

Fig. 15. Stress (a), displacement (b) and strain (c) of stained-glass window

The most important element of the research carried out in this study was to determine whether the bell does not generate vibration frequencies close to the resonance frequencies of the proposed models (glass only, simplified stained-glass and full stained-glass Therefore, Table 8 presents the numerical partials of the sound and the vibration frequencies of the stained-glass window closest to these values with the mode number (in brackets). On this basis, it can be concluded that a stained-glass window with a glass thickness of 3 mm is most exposed to the resonance phenomenon, because the vibration frequency values 50, 63 and 205 practically coincide with the bell sound partials. In other cases, the analyzed bell should not cause any negative mechanical effects on the stained-glass window.

Table 8. Comparison of the vibration frequencies of the bell and the stained-glass window.

Frequency of bell	Thickness of glass (a) [mm]			
	3	4	5	6
	Frequency [Hz] (No. of mode)			
589.99	593.87 (23)	584.84 (16)	575.73 (12)	597.36 (10)
1185.8	**1184.90** (50)	1188.00 (37)	1202.40 (29)	1171.60 (22)
1413.9	**1414.30** (63)	1405.00 (46)	1417.50 (34)	1443.40 (29)
1773.8	1765.20 (80)	1784.20 (59)	1758.70 (46)	1784.20 (37)
2376.5	**2378.40** (205)	2385.40 (81)	2367.80 (63)	2388.10 (50)

Conclusions

In this work, a number of numerical and experimental studies were carried out. The first stage was reverse engineering [18], i.e. scanning an actual bell in one of the churches in Lithuania and developing its rib on this basis. The transverse profile of the bell allowed the preparation of a scaled numerical model. This model and its acoustic properties and impact on nearby objects were analyzed in the ANSYS program.

The numerical model of the bell was also used in the second stage of the research. On its basis, foundry molds were prepared, which were printed from sand and resin and a physical object was cast in them. The casted bell was experimentally tested to obtain vibration frequencies and SPL.

The next stage of the work was an advanced analysis of two models of the stained-glass window and the glass itself. The frequencies and vibration modes of the analyzed models were obtained and compared with the acoustic properties of the considered bell.

The get results allowed us to conclude that the acoustic force generated by the bell itself will not have a negative impact on a stained-glass window even in its close vicinity. However, resonance frequencies may have an adverse effect. Therefore, when designing stained-glass windows, it is necessary to analyze the partials of the sound of the bell, which will be located nearby and directly affect the stained glass window, as well as the natural vibrations of the stained-glass window. If it occurred between the above frequency correlation, it would be necessary to select the appropriate glass thickness or possibly reduce or increase the number of lead cames, which causes the resonance frequencies to increase or decrease, respectively.

An additional aspect that will be taken into account in subsequent tests is the impact of vibrations generated during the ringing of bells, in the structure supporting the bell, and transmitted to the floor/walls/ceiling (depending on the method of mounting the bell), and then to the walls and windows [19, 20, 21].

Acknowledgments

This publication was financed by the Ministry of Science and Higher Education of Poland as the statutory financial grant of the Department of Mechanics and Machine Design Fundamentals of Czestochowa University of Technology.

The authors are grateful to for granting access to the computing infrastructure built in the projects No. POIG.02.03.00-00-028/08 "PLATON - Science Services Platform" and No. POIG.02.03.00-00-110/13 "Deploying high-availability, critical services in Metropolitan Area Networks (MAN-HA)"

References

[1] W. Ślesiński, *Conservation of stained-glass windows*, **Ochrona Zabytków**, **46/4**(183), 1993, pp. 328-337 (in Polish).

[2] A.M. Corrêa Pinto, M.F. Macedo, M.G. Vilarigues, *The conservation of stainedglass windows in Latin America: a literature overview*, **Journal of Cultural Heritage**, **34**, 2018, pp. 172-181, https://doi.org/10.1016/j.culher.2018.04.019.

[3] F.C. Pizano, *Study of the medieval lead cames used in the stained glass windows of the Monastery of Pedralbes (Barcelona)*, **Materíales de Construcción**, **259**, 2000, pp. 85-95, https://doi.org/10.3989/mc.2000.v50.i259.401.

[4] D. Koga, E. Morasset, R. Pepi, D. Woodham, *Protecting Stained-Glass Windows from Vibrations Caused by Construction Operations*, **APT Bulletin: The Journal of Preservation Technology**, **51**(4), Special Issue: Mitigating Vibration Damage, 2020, pp. 6-12, https://www.jstor.org/stable/10.2307/26970187.

[5] A. Gregorini, S. Paganoni, E. Zappa, A. Cigada, F. Canali, *Effects of environmental vibration on ancient stained-glass windows*, **Journal of Cultural Heritage**, **56**, 2022, pp. 65–74, 10.1016/j.culher.2022.06.002.

[6] C.Q. Howard, B.S. Cazzolato, *Acoustic Analyses Using MATLAB and ANSYS*, **CRC Press Taylor & Francis Group**, 2015.

[7] H.H. Lee, *Finite Element Simulations with ANSYS Workbench 2023*, **SDC Publications**, 2023, ISBN: 978-1-63057-615-8.

[8] C. Xiaolin, L. Yijun, *Finite Element Modeling and Simulation with ANSYS Workbench*, **Taylor & Francis Ltd**, 2018, DOI: https://doi.org/10.1201/9781351045872.

[9] E.M. Alawadhi, *Finite Element Simulations Using ANSYS,* **Apple Academic Press Inc**, 2015, https://doi.org/10.1201/b18949.

[10] J.E. Akin, *Finite Element Analysis Concepts: Via SolidWorks*; **World Scientific: Hackensack**, NJ, USA, 2010, DOI:10.1142/7785.

[11] R. Shih, *Introduction to Finite Element Analysis Using SOLIDWORKS Simulation 2021*, **SDC Publications**, 2021.

[12] D. Cekus, M. Nadolski, *Assessment of the change in the tin concentration in bronzes to the basic components of the sound of bells*, **Archives of Metallurgy and Materials**, **66**, 2021, pp. 531-535, https://doi.org/10.24425/amm.2021.135889.

[13] N. Xiang, J. Blauert, *Acoustics for Engineers*, **Springer**, 2021.

[14] R. Perrin, T. Charnley, G. Swallowe, *On the tuning of church and carillon bells*, **Applied Acoustics**, **46**(1), 1995, pp. 83-101, https://doi.org/10.1016/0003-682X(95)93952-E.

[15] T.D. Rossing, R. Perrin, *Vibrations of bells*, **Applied Acoustics**, **20**(1), 1987, pp. 41-70, https://doi.org/10.1016/0003-682X(87)90082-X.

[16] D. Cekus, P. Kwiatoń, M. Nadolski, K. Sokół, *Effect of material-technological properties on the reconstruction of utility parameters of bells*, **Engineering Science and Technology, an International Journal**, **24**(4), 2021, pp. 1042-1048, https://doi.org/ 10.1016/j.jestch.2021.01.012

[17] D. Cekus, P. Kwiatoń, M. Nadolski, K. Sokół, *Quality Assessment of Manufactured Bell Using 3D Scanning Process*, **Sensors**, 20(24), 2020, p.7057, DOI:10.3390/s20247057.

[18] K. Sokół, D. Cekus, *Reverse engineering as a solution in parts restoration process*, **Procedia Engineering**, **177**, 2017, pp. 210-217, https://doi.org/10.1016/j.proeng. 2017.02.191.

[19] K. Gromysz, Ł. Drobiec, Z. Pająk, *Some aspects of building new bells in the Mariacki church tower in Katowice*, **Czasopismo Techniczne. Budownictwo**, R. 106, Z. 9, 2-B, 2009, pp. 97-108 (in Polish).
[20] J.M. Wilson, A.R. Selby, S.E. Ros, *The dynamic behaviour of some bell towers during ringing*, **Transactions on the Built Environment**, **4**, 1993, pp. 491-500, ISSN 1743-3509.
[21] E.E. Smirnova, S.N. Savin, D.V. Larin, *Research of influence of vibration impacts of chimes on the steeples of St. Isaac's Cathedral (Saint Petersburg) after reconstruction thereof*, **MATEC Web of Conferences**, **285**, 00017, 2019, DOI:10.1051/ MATECCONF/201928500017.

Received: June 02, 2023
Accepted: May 20, 2024